J. Appl. Comput. Mech., 11(3) (2025) 692-706
DOI: 10.22055/jacm.2024.47488.4725

ISSN: 2383-4536
jacm.scu.ac.ir

Shahid Chamran University of Ahvaz

Journal of Applied and Computational Mechanics

Research Paper

Optimization and Sensitivity Analysis of Location Parameters in Heating and Cooling Systems for Minimizing Suspended Particles in an Enclosed Environment

Hasan Sajjadi[1], S. Nader Nabavi[1], Amin Amiri Delouei[1,2], Meysam Atashafrooz[3], Mohammad Mehdi Rashidi[4]

[1] Department of Mechanical Engineering, University of Bojnord, Bojnord, Iran,
Email: h.sajjadi@ub.ac.ir (H.S.); s.nader.nabavi@ub.ac.ir (S.N.N.); a.amiri@ub.ac.ir (A.A.D.)

[2] Department of Mechanical Engineering, Lakehead University, Thunder Bay, Canada, Email: aadeloue@lakeheadu.ca

[3] Department of Mechanical Engineering, Sirjan University of Technology, Sirjan, Iran, Email: m.atashafrooz@sirjantech.ac.ir

[4] University of Electronic Science and Technology of China, Chengdu, 610054, Sichuan, P.R. China, Email: mm_rashidi@yahoo.com

Received July 19 2024; Revised September 25 2024; Accepted for publication October 04 2024.
Corresponding author: H. Sajjadi (h.sajjadi@ub.ac.ir, hsajjadi@clarkson.edu)

Abstract. To analyze how temperature distribution affects particle deposition in an enclosed space, different placements for heating and cooling systems (HC) are examined and the quantity of particles deposited is determined. Taguchi's optimization method is implemented for finding the best location in order to reduce the number of suspended particles. To evaluate the effect of particle size on the deposition rate for various HC system locations, particles with different sizes (100 nm to 10 µm) are considered. With respect to the results, the location of the HC system does not have a significant effect on the deposition rate of small-sized particles (1 µm and 100 nm), but for particles with a size of 10 µm, where the most of the Covid-19 and Sars viruses are in this range, the HC system's location significantly affects the number of suspended particles. Therefore, the optimization process with Taguchi's method has been carried out for the particle with a size of 10 micrometers. Furthermore, the findings indicate that the vertical placement of the heater system is the most important factor and the longitudinal position of the cooler system is the least important factor in the reduction of suspended particles.

Keywords: Suspended particles; HC location; LBM; Taguchi's optimization method; Sensitivity Analysis.

1. Introduction

As a result of particles expelled during human respiration, SARS-Covid and other respiratory viruses are likely to be transmitted among infected people [1, 2]. The rate of transmission and deposition of the particles and droplets depends on their size and type, and for small particles, it is possible to transfer to long distances [3, 4]. On the other hand, when the HC system is on in an enclosed space, its position can have an important effect on how the viruses are transmitted. This effect can be positive for reducing the level of contamination of people or negative for increasing the level of contamination of people. So that if an infected person sneezes or coughs in an enclosed space, the viruses will be suspended in the air, and if the HC system is well placed, the rate of their settling in short distances can be increased and the number of suspended particles will be declined [5, 6].

The experimental investigation of indoor flows and also the experimental observation of the particles motion such as viruses are very complicated and expensive, therefore, numerical modeling of such problems has caught the interest of scholars [7-10]. The Lattice Boltzmann method (LBM), as one of the well-known methods for complex geometries and investigating the behavior of particles with different sizes has been used by many researchers in the past decades [11, 12]. Sajjadi et al. [13] investigated the deposition and dispersion of particles inside an office room. They used the LBM to analyze the flow and particles motion and reported that the LBM as an efficient and low-cost method can well predict the behavior of particles. Also, recently Sajjadi et al. [4], analyzed the effect of the inlet air location on the transfer and settling of incoming particles by the air conditioning system using the LBM. Their findings indicated that the position of the inlet air can have a great effect on increasing or decreasing the transfer rate of pollutants. Zhao et al. [14] investigated the behavior of particles from sneezing and coughing inside the room. The geometry that they investigated was a simple room in which a person sneezes. Their results showed that during normal breathing, a small number of particles enter the environment, and the entered particles also travel a very small distance. But when the person coughs or sneezes, a much larger number of particles enter the environment and there is a possibility of transmission up to more than 3

Published online: October 27 2024

meters. Liu and Novoselac [15] modeled an artificial cough and reported the results of analytical and experimental solutions. Their results showed that the size of the particles is very effective in the amount of transmission, so that for large particles with a size of 7 micrometers, the amount of transmission is very small and after a few millimeters, they deposited on the ground, but for small particle with a size of about one micrometer this distance increases to about one meter. Ahmadzadeh and Shams [16] introduced a numerical method to prevent the spread of infectious diseases in the meeting room. They used ANSYS Fluent software to analyze the motion of particles produced inside a safe meeting room. Their purpose was to consider the effects of window opening frequency, outlet layout and position of AC systems on particle motion. Their results illustrated that the fraction of particles which are in the room will decrease by more than 35% and the number of people who are exposed to the contamination of viral particles will declined three times. Motosamy et al. [17] investigated the impact of cough pattern on appropriate social distance in an enclosed space. They numerically examined the evolution of transient cough, contamination range, probability of particle arrival and deposition fraction for different age groups of men and women while standing and sitting in a ventilated room. The results showed that, in general, the range of contamination is lower for women due to the speed of coughing and the number of particles. In addition, a significant part of the particles passes the two-meter threshold of social distancing by coughing without hindrance.

In many engineering problems, finding optimum values for problem parameters in order to achieve a desired goal is one of the challenges in designing systems. Various algorithms have been devised to find the optimal values of a problem. In some cases, to find optimal values, an analytical solution can be found using the first and second derivatives of the objective function [18]. There are also scientific methods such as OFAT [19] and trial and error methods [20], which are usually time-consuming to implement. In fact, such methods require a large number of unnecessary experiments, which is practically an inefficient method. In addition to traditional optimization methods, there are other optimization methods called evolutionary algorithms. These algorithms generate answers randomly in the initial steps and produce better answers in later steps by relying on natural processes [21, 22]. On the other hand, design of experiments (DOE) is a statistical technique that aims to identify which factors significantly affect the output of a system. DOE involves designing an experiment by systematically varying the levels of input variables and measuring the outcomes. By analyzing the data using statistical tools, engineers can determine the effect of each variable and optimize the system accordingly. DOE methods achieve more reliable results, save time, significantly reduce the number of experiments and ultimately lead to process optimization. One of the methods of designing experiments in order to determine the optimal combination of parameters is to examine all possible combinations of variable levels (full factorial) and find the optimal combination among them [23]. Finding the optimal combination of the full factorial of experiments is reasonable, but not cost-effective in terms of time and cost. Taguchi's method [24, 25], widely used in various branches of engineering [26, 27], is known as a fractional factorial method in the DOEs. In the orthogonal array, all parameters are examined simultaneously, and it may also be possible to examine the interaction effect of the parameters. Among the advantages of Taguchi's method, it can be mentioned the reduction of the number of experiments and costs and the possibility of examining qualitative or quantitative parameters with different levels. In Taguchi's method, the concept of signal-to-noise (SN) ratio is used to obtain optimal conditions in the DOEs. A high SN value indicates that the effect of controllable parameters is greater than the effect of uncontrollable parameters or disturbance parameters [28].

According to the literature review, it is very important to investigate the effect of the location of HC systems on the particles deposition. To the best of our knowledge, no research has been done on the effect of the location of heating systems which are based on natural heat convection on the particles motion. Therefore, here, the effect of these types of heating systems location on the particles deposition is investigated, and the best location to reduce the amount of suspended particles for different sizes (100 nm to 10 micrometers) is obtained using the Taguchi`s method for the first time.

2. Present Geometry

The current research deals with the study of a three-dimensional cubic office room with a natural convection based HC system (Fig. 1). In order to optimize the position of the HC system to reduce the number of suspended particles, it has been decided to select sixteen different positions. In this arrangement, the wall located at X = 0, contains a two dimensional (L/4 × L/4) heater and the wall located at X = L, contains a two dimensional (L/4 × L/4) cooler. H_H and L_H are used to show the position of the heater and H_C and L_C for the cooler. The constant temperature boundary condition is utilized for the HC system and the adiabatic is utilized for other walls. Also, the flow is incompressible and the Boussinesq approximation is utilized. To consider the effect of buoyancy force two Rayleigh numbers (Ra = 10^4 and Ra = 10^5) were chosen. Also, for investigating the particle motion, 64000 particles with three different sizes (100 nm, 1 μm and 10 μm) are injected in the middle of the room and the behavior of them have been tracked for 100s after injection. Particles are deposited when they touch each of the walls.

Based on the present geometry and natural convection heat transfer, the governing equations in non-dimensional form are derived as follows:

$$\frac{\partial V}{\partial Y}+\frac{\partial W}{\partial Z}+\frac{\partial U}{\partial X}=0 \tag{1}$$

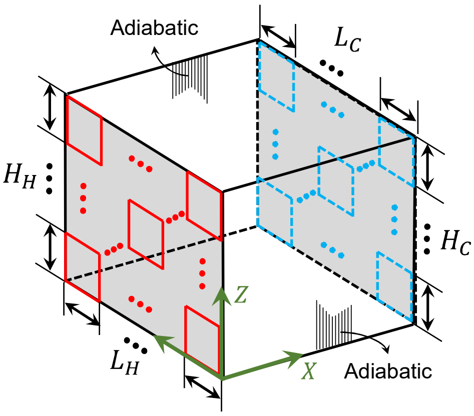

Fig. 1. Schematic of the proposed geometry.

$$\frac{\partial U}{\partial t}+V\frac{\partial U}{\partial Y}+W\frac{\partial U}{\partial Z}+U\frac{\partial U}{\partial X}=-\frac{\partial P}{\partial X}+\Pr(\frac{\partial^2 U}{\partial Y^2}+\frac{\partial^2 U}{\partial Z^2}+\frac{\partial^2 U}{\partial X^2}) \tag{2}$$

$$\frac{\partial V}{\partial t}+V\frac{\partial V}{\partial Y}+W\frac{\partial V}{\partial Z}+U\frac{\partial V}{\partial X}=-\frac{\partial P}{\partial Y}+\Pr(\frac{\partial^2 V}{\partial Y^2}+\frac{\partial^2 V}{\partial Z^2}+\frac{\partial^2 V}{\partial X^2}) \tag{3}$$

$$\frac{\partial W}{\partial t}+V\frac{\partial W}{\partial Y}+W\frac{\partial W}{\partial Z}+U\frac{\partial W}{\partial X}=-\frac{\partial P}{\partial Z}+\Pr(\frac{\partial^2 W}{\partial Y^2}+\frac{\partial^2 W}{\partial Z^2}+\frac{\partial^2 W}{\partial X^2})+Ra\Pr T \tag{4}$$

$$\frac{\partial T}{\partial t}+V\frac{\partial T}{\partial Y}+W\frac{\partial T}{\partial Z}+U\frac{\partial T}{\partial X}=(\frac{\partial^2 T}{\partial Y^2}+\frac{\partial^2 T}{\partial Z^2}+\frac{\partial^2 T}{\partial X^2}) \tag{5}$$

3. Numerical Solution

The Lattice Boltzmann method (LBM) is an efficient computational method used to simulate the flow of fluids. It is particularly well-suited for the simulation of natural or forced convection problems. The main advantages of the LBM compared to other numerical methods can be listed as follows:

1. It is a Lagrangian approach, which allows for the study of arbitrary shaped domains.
2. It is a meshless method, which eliminates the need for a complex and time-consuming grid generation process.
3. It can accurately capture flow phenomena such as shocks, complex geometries and contact lines.
4. It is computationally efficient and can be easily parallelized for improved performance.
5. It is highly versatile and used to simulate a vast variety of natural phenomena.

Therefore, this method is used to solve the flow filed.

3.1. Double multi relaxation Lattice Boltzmann method (DMRT-LBM)

The Multi Relaxation Time (MRT) technique has several benefits for the collision step of Lattice Boltzmann Method (LBM). These advantages primarily comprise of enhanced stability, greater precision, quicker convergence, reduced storage needs, and improved parallelism [11-13].

In comparison to single relaxation time (SRT) method, the MRT technique exhibit a greater degree of stability, thereby allowing for an increase in the time step size that ultimately results in a faster and more precise solution. This enhanced stability can be attributed to the MRT method having superior numerical diffusion characteristics, which in turn leads to improved numerical stability. Additionally, the MRT method offers superior convergence properties compared to the SRT method, as they require fewer iterations to achieve a steady-state solution, thus reducing computational costs.

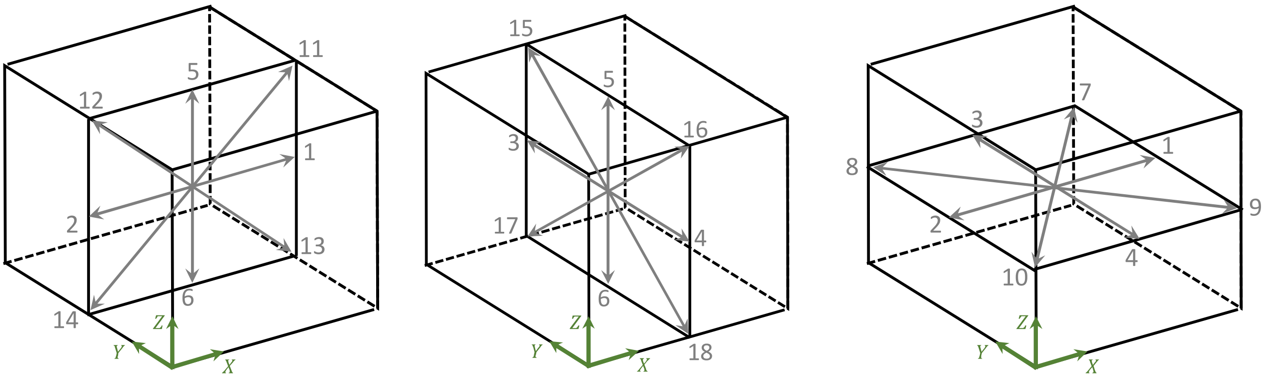

Fig. 2. The D3Q19 lattice.

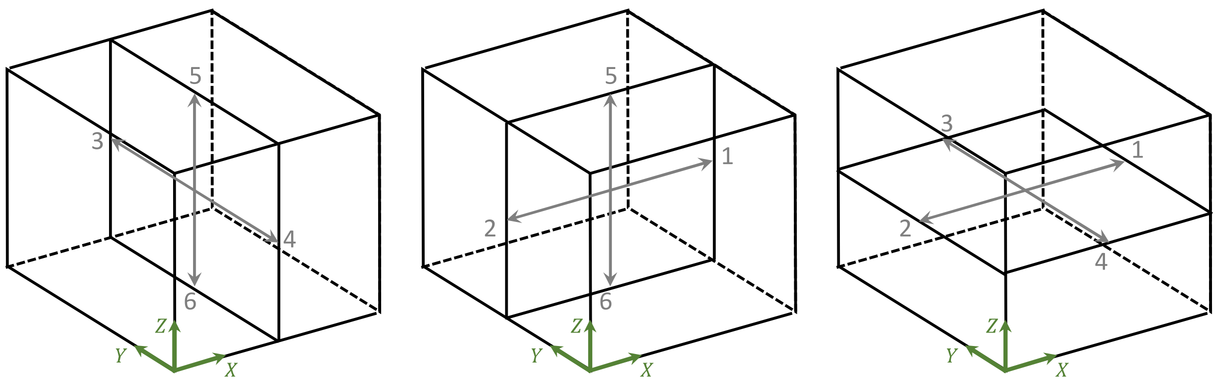

Fig. 3. The D3Q7 lattice.

The MRT method was employed in this study due to its exceptional stability. Using this method and considering the D3q19 lattice (Fig. 2) for flow and D3Q7 lattice (Fig. 3) for temperature fields, the equations for temperature and velocity distribution functions are presented as below:

$$f_i(x + c_i\Delta t, t + \Delta t) = f_i(x,t) - M_{ij}^{-1}.\hat{S}_{jk}.[R_k(x,t) - R_k^{eq}(x,t)] + F_i \tag{6}$$

$$h_i(x + e_i\Delta t, t + \Delta t) = h_i(x,t) - N_{ij}^{-1}.\hat{Q}_{jk}.[n_k(x,t) - n_k^{eq}(x,t)] \tag{7}$$

In Eqs. (6) and (7), c_i and e_i represent the discrete speed of particles, which are expressed as follows for the D3Q19 and D3Q7 lattices:

$$c_i = \begin{cases} (0,0) & i=0 \\ c(\pm1,0,0), c(0,\pm1,0), c(0,0,\pm1) & i=1-6 \\ c(\pm1,\pm1,0), c(\pm1,0,\pm1), c(0,\pm1,\pm1) & i=7-18 \end{cases} \quad \text{for} \quad D3Q19 \tag{8}$$

$$e_i = \begin{cases} 0 & i=0 \\ e(\pm1,0,0) & i=1,6 \\ e(0,\pm1,0) & i=3,4 \\ e(0,0,\pm1) & i=5,6 \end{cases} \quad \text{for} \quad D3Q7 \tag{9}$$

Details of the Eqs. (6) and (7) such as M_{ij}^{-1} and N_{ij}^{-1} have been reported in [29], so they were not explained in this work.

3.2. Particle motion equation

The movement of particles can be explained using the subsequent formula [30]:

$$\frac{du_i^p}{dt} = \frac{1}{\tau_p}\frac{C_D \mathrm{Re}_p}{24}(u_i - u_i^p) + (1 - \frac{1}{s})g_i + n_i(t) \tag{10}$$

Here u_i^p, g_i, and $n_i(t)$, are the particle velocity, the accelerations of the body forces and the Brownian force per unit mass, respectively. $\tau_p = Sd^2C_C / 18\nu$ is known as particle relaxation time, where particle density divided by fluid density is defined by S, and $C_c = 1 + 2\lambda(1.257 + 0.4\exp(-1.1d/\lambda))/d$ is the Stokes-Cunningham slip correlation. Using the equations below, drag coefficient can be obtained:

$$C_D = \frac{24}{\mathrm{Re}_p} \qquad \mathrm{Re}_p < 1 \tag{11}$$

$$C_D = \frac{24}{\mathrm{Re}_p}(1 + 0.15\mathrm{Re}_p^{0.687}) \qquad 1 < \mathrm{Re}_p < 400 \tag{12}$$

$$\mathrm{Re}_p = \frac{d|u_{rel}|}{\nu} \qquad u_{rel} = u_j - u_j^p \tag{13}$$

Among small particles, Brownian force $n_i(t)$ is important, and reported as follows [13]:

$$n_i(t) = \zeta_i\sqrt{\frac{216\pi\nu k_b T}{\Delta t\pi^2\rho d^5 S_0^2 C_c}} \tag{14}$$

3.3. Taguchi's method

Optimization with Taguchi's method is an effective approach to solving complex problems that require many variables to be optimized simultaneously. In contrast to other techniques for evolutionary optimization, like particle swarm optimization and genetic algorithms, Taguchi optimization evaluates a set of predetermined values and parameters to determine how an outcome is affected. This is done by running a series of experiments with different parameters that designed by orthogonal arrays. The design of experiments using the orthogonal array technique reduces the number of experiments as much as possible.

In order to use the Taguchi method, first, the parameters affecting the desired process and their different levels should be determined. Then, the minimum number of experiments is designed using orthogonal arrays. After the experiments, the results are compared with each other in order to determine the appropriate level of each parameter to achieve the goal of the problem. One of the available tools for analyzing the results of experiments is the signal-to-noise (SN) ratio.

The SN ratio, is a key parameter in Taguchi's method. It is used to measure the performance of a product and is calculated by comparing the desired output signal to the undesired output noise. In Taguchi's method, the SN ratio is used to compare the difference between the actual performance and the desired performance.

To determine the SN ratio, according to the purpose of the problem, three functional characteristics "smaller value is best", "larger value is best" and "nominal value is best" can be used. In Eqs. (15) to (17), the method of calculating the SN ratio is given according to the three introduced performance characteristics, respectively.

$$S/N = -10\log(\frac{1}{n}\sum_{i=1}^{n} y_i^2) \tag{15}$$

$$S/N = -10\log\left(\frac{1}{n}\sum_{i=1}^{n}\frac{1}{y_i^2}\right) \tag{16}$$

$$S/N = -10\log\left(\frac{1}{n}\sum_{i=1}^{n}(y_i - y_0)^2\right) \tag{17}$$

in which S/N is the SN ratio, n is the number of repetitions of each experiment, y_i is the desired output and y_0 is the target value. It should be noted that in order to determine the optimal value of each parameter, the level with the highest SN ratio is closer to the goal of the problem and is the optimal level of the parameter.

The factors studied in this research are H_H, L_H, H_C and L_C and four levels are considered for each factor. Table 1 shows all the factors and their corresponding levels.

According to the factors number (#4) and the levels number of each parameter (#4), the proper orthogonal array to determine the design of experiments is L_{16} that is given in Table 2.

Taguchi's method is one of the powerful optimization tools that has recently been widely used in various engineering systems. Compared to other common methods, the special advantage of this method is to decline the number of experiments and minimize changes around the target through process optimization. Therefore, the computation time and the cost in this method are significantly reduced. It is also possible to consider the impact of several variables on a process with the least number of experiments using this method.

4. Results and Discussion

4.1. Grid study and code validation

The numbers of deposited 1 μm particles after 100 s for the number of experiment 2 and Ra = 10^4 are shown for different grid sizes in Fig. 4. Two consecutive grid resolutions (60×60×60) and (70×70×70) showed little variation for the particle deposition, as a result, the (60×60×60) grid size was selected.

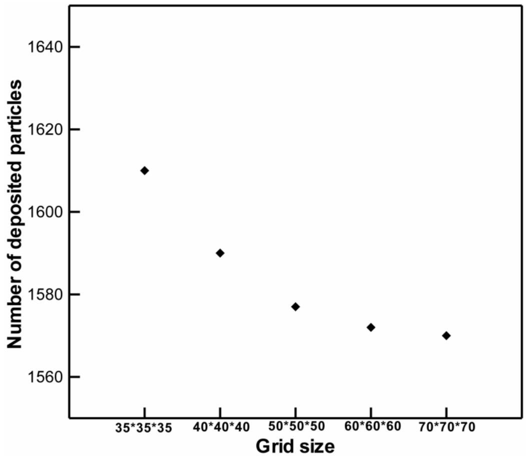

Fig. 4. Grid independency.

Table 1. Factors and levels in Taguchi analysis.

System	Factors		Levels 1	2	3	4
Heater	Height position	H_H	$X = 0.00$ $0.00 < Z < 0.25$	$X = 0.00$ $0.25 < Z < 0.50$	$X = 0.00$ $0.50 < Z < 0.75$	$X = 0.00$ $0.75 < Z < 1.00$
	Longitudinal position	L_H	$X = 0.00$ $0.00 < Y < 0.25$	$X = 0.00$ $0.25 < Y < 0.50$	$X = 0.00$ $0.50 < Y < 0.75$	$X = 0.00$ $0.75 < Y < 1.00$
Cooler	Height position	H_C	$X = 1.00$ $0.00 < Z < 0.25$	$X = 1.00$ $0.25 < Z < 0.50$	$X = 1.00$ $0.50 < Z < 0.75$	$X = 1.00$ $0.75 < Z < 1.00$
	Longitudinal position	L_C	$X = 1.00$ $0.00 < Y < 0.25$	$X = 1.00$ $0.25 < Y < 0.50$	$X = 1.00$ $0.50 < Y < 0.75$	$X = 1.00$ $0.75 < Y < 1.00$

Table 2. Table of Taguchi experiments based on L_{16} orthogonal array.

Number of Exp.	Factors H_H	L_H	H_C	L_C	Number of Exp.	Factors H_H	L_H	H_C	L_C
1	1	1	1	1	9	3	1	3	4
2	1	2	2	2	10	3	2	4	3
3	1	3	3	3	11	3	3	1	2
4	1	4	4	4	12	3	4	2	1
5	2	1	2	3	13	4	1	4	2
6	2	2	1	4	14	4	2	3	1
7	2	3	4	1	15	4	3	2	4
8	2	4	3	2	16	4	4	1	3

Table 3. Nusselt number comparison with Khanafer et al. [31].

Rayleigh number	Present work	Khanafer et al. [31]
10^3	1.85	1.96
10^4	4.02	4.03
10^5	8.10	8.31

As it is mentioned in the literature review there is not any data for particle motion in a closed room with a natural based HC systems, so to confirm the results which are achieved from a homemade FORTRAN code, a comparison of the Nusselt number at different Rayleigh numbers with the findings from a previous study [31] is displayed in Table 3. Approximately 5% errors were observed in the present study, which would be acceptable.

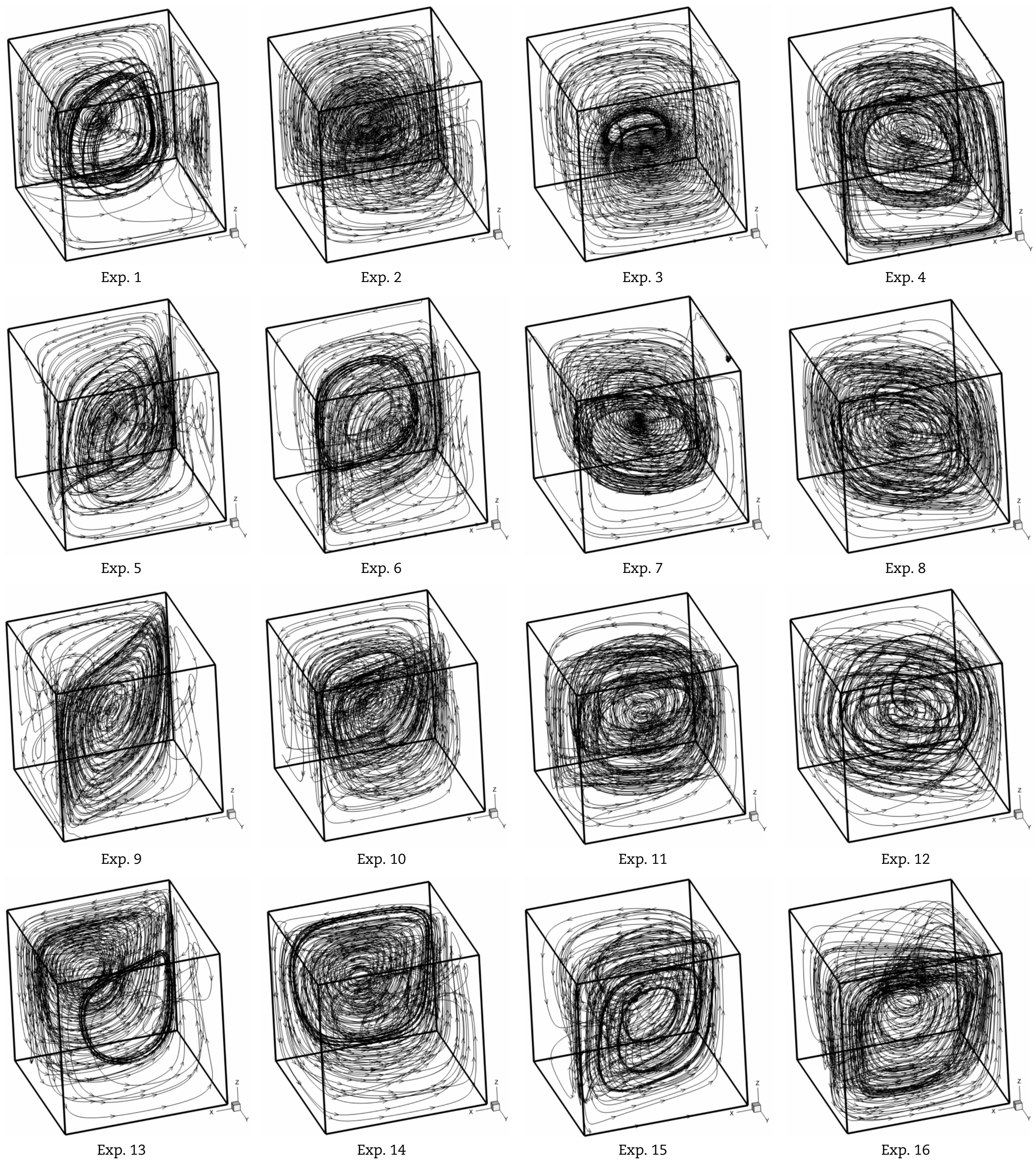

Fig. 5. Streamline for Ra = 10^4 and various experiment numbers.

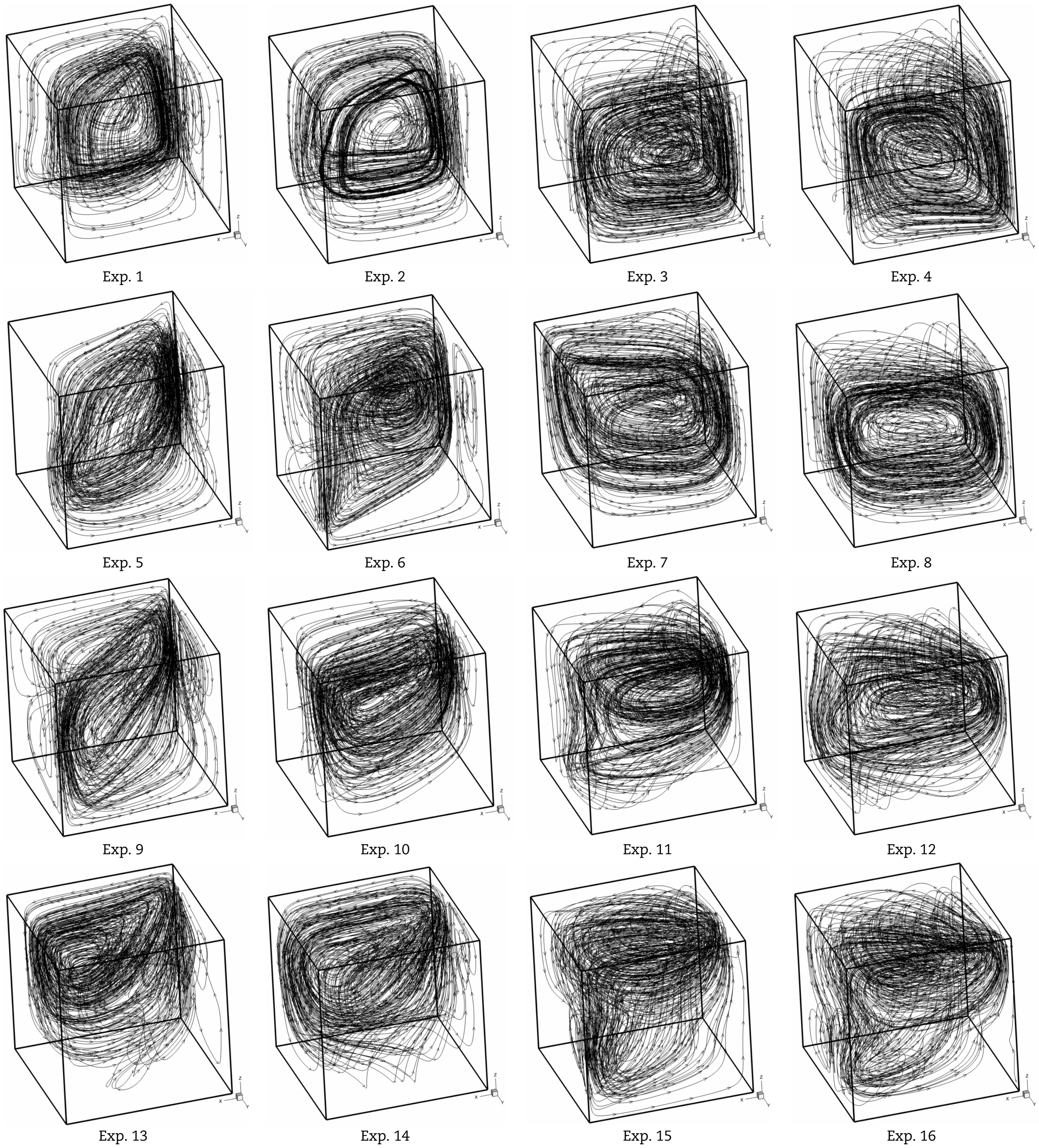

Fig. 6. Streamline for Ra = 10^5 and various experiment numbers.

4.2. Flow pattern

Particle motion in laminar natural convection is greatly affected by the flow pattern. As the flow pattern affects the forces acting on individual particles, the particle trajectories, velocities and microstructure of the medium, it affects the motion of the particles. For instance, if the flow pattern is laminar, the forces on the particles are symmetrical, resulting in a straight-line motion along the flow axis. On the other hand, if the flow pattern is turbulent, it leads to a more complex motion of the particles, with the particles being pulled in multiple directions. Therefore, the flow pattern has a significant influence on the particle motion in laminar natural convection. So, in this work the streamlines are presented for the various experiments in Figs. 5 and 6 for Ra = 10^4 and Ra = 10^5, respectively. As it is observable in Figs. 5 and 6, by changing the position of HC system the streamlines changed significantly, especially for Ra = 10^5. The flow pattern in natural convection heat transfer is significantly influenced by the Rayleigh number. As the Rayleigh number increases, the fluid motion changes from a laminar flow to a turbulent flow, this change in flow pattern is accompanied by a change in the streamlines. At low Rayleigh number (Ra = 10^4), the streamline pattern is smooth and regular, and the fluid motion is dominated by conduction. As the Rayleigh number increases, the fluid motion becomes more turbulent and chaotic, with convection dominating, and streamlines becoming increasingly complex and irregular. Additionally, eddies and vortices form within the flow.

Table 4. Number of deposited particles on the room walls for Ra = 10^4.

Number of Experiment	1 µm	10 µm	100 nm
1	1579	52643	187
2	1577	50215	205
3	1576	48967	198
4	1579	50795	230
5	1602	50901	186
6	1601	51098	202
7	1601	49285	188
8	1601	49387	203
9	1601	50903	203
10	1601	50070	229
11	1604	52363	209
12	1601	51822	170
13	1601	52799	172
14	1601	52332	179
15	1603	52840	162
16	1601	54058	175

Table 5. Number of deposited particles on the room walls for Ra = 10^5.

Number of Experiment	1 µm	10 µm	100 nm
1	1592	43186	278
2	1600	40207	292
3	580	38720	278
4	1575	40744	255
5	1689	44509	279
6	1664	43304	263
7	1660	40580	268
8	1667	42579	230
9	1650	46135	238
10	1660	45826	219
11	1676	49551	221
12	1680	48358	205
13	1637	49930	242
14	1642	49123	263
15	1660	50137	266
16	1650	52021	254

4.3. Particle deposition

Particles are deposited on the walls of a room in a few different ways. The most common is via air circulation. As air moves through the room, some of the particles suspended in the air will be deposited on the walls and other surfaces. Particles can also be deposited by direct contact, this occurs when something is physically brought into the room, such as clothing, furnishings, or animals, which can carry particles from the outside environment. Particles can also be created within the room, such as from cooking, burning, or chemical reactions. In this work, the air circulation effect on particle deposition has been investigated. Big particles such as dust, pollen and other allergens tend to fall to the floor due to gravity. This is because they are heavier than the air molecules that surround them, so they are pulled downward by the force of gravity. These particles can also be pushed down to the floor by air currents, such as the air being expelled from a fan or an air conditioner. Small particles suspended in a room remain afloat due to their low mass and the force of air currents, this is known as Brownian motion. Unlike larger particles, smaller particles cannot overcome the force of air currents, causing them to remain suspended in the air.

In this research, based on Taguchi experiments, the number of deposited particles on the room walls for different Rayleigh numbers have been investigated and the results are given in Tables 4 and 5. (More details have been reported in Appendix A).

To show the pattern of deposition on the walls of the room for various experiments visually, Figs. 7 and 8 show the walls that the particles are deposited on them for different experiment numbers (To brevity some of the cases are illustrated).

By increasing the size of the particles, the deposition rate will increase for all positions of the HC system and also for both Rayleigh numbers, and most of the particles will deposit on the floor of the room. This result is obvious because as the size of the particle increases, its mass increases, as a result, the buoyancy force will become the dominant force and the particles will deposit toward the floor of the room in the direction of this force. In addition, it was observed that the tendency of the small particles (100 nm and 1 µm) to move towards the positions of the HC system is greater and they deposited on the left wall (X = 0).

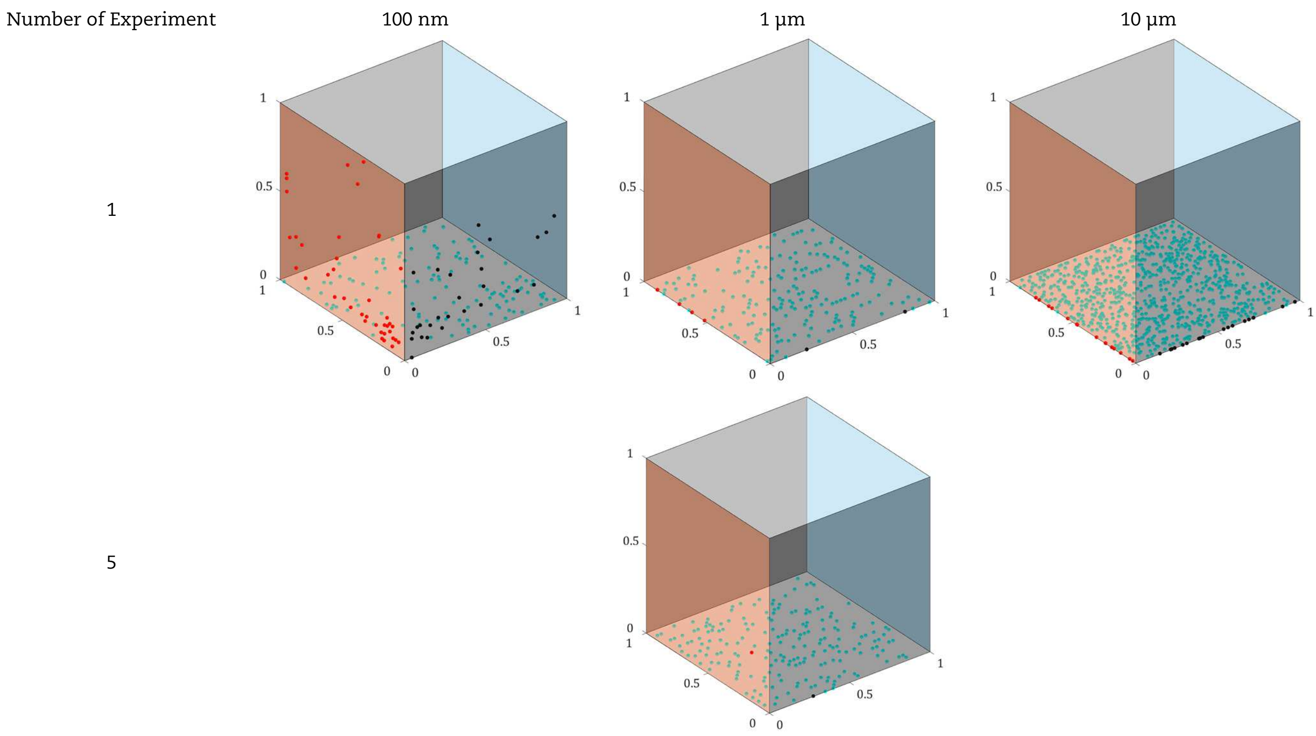

Fig. 7. Deposited particles on the room walls for Ra = 10^4.

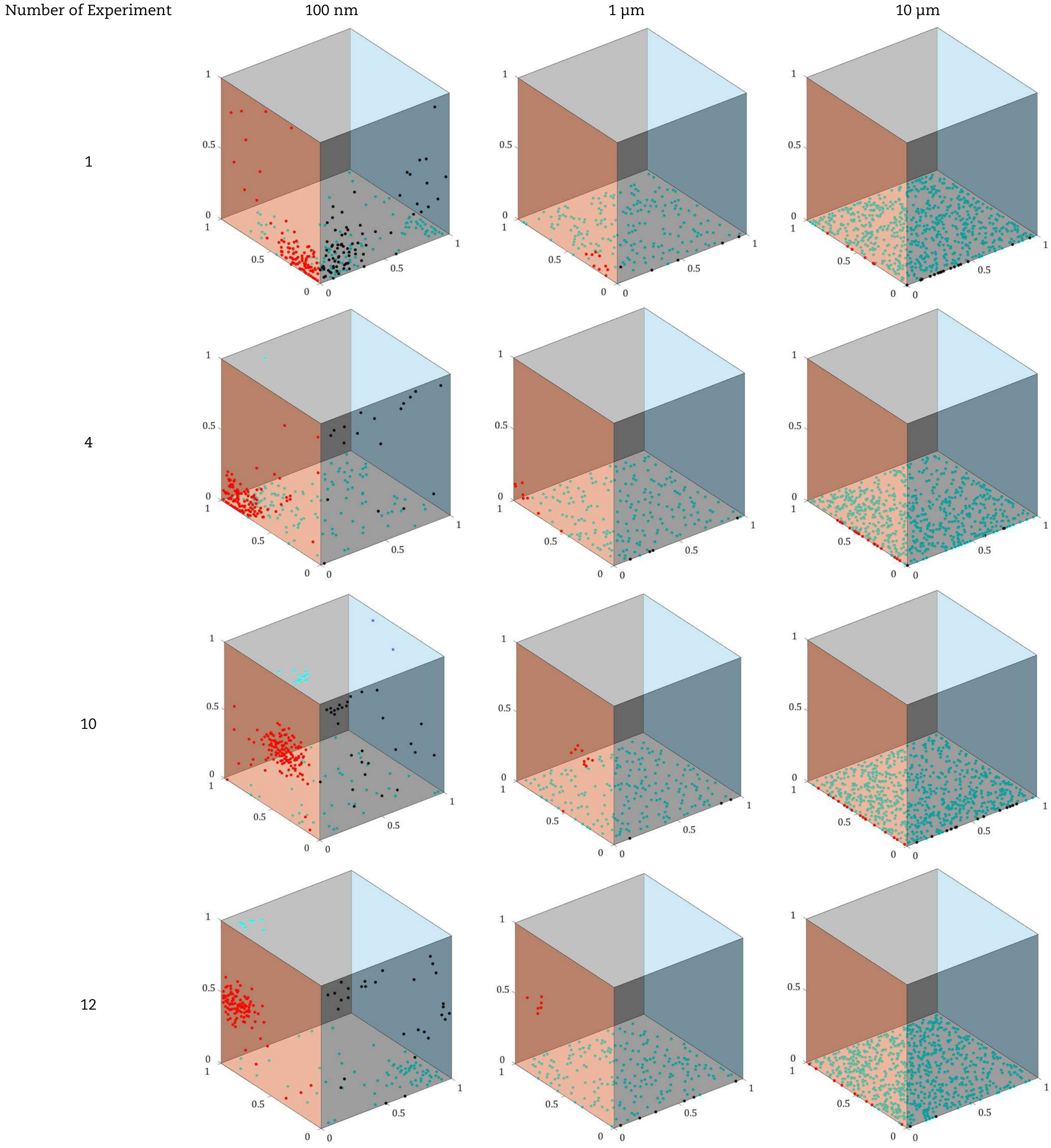

Fig. 8. Deposited particles on the room walls for Ra = 10^5.

For particles with the smallest size (100 nm), as can be seen in Figs 7 and 8, due to the low mass of these particles, the Brownian force will be the dominant force and the particles will be more affected by the flow, so according to the Fig. 5 and 6 that show the flow path, by changing the position of the HC system, the dispersion path of these particles is affected more than large particles, and they remain suspended inside the room and deposited less than bigger size on the walls.

Deposition on the upper wall (Z = H), the front wall (Y = L), the back wall (Y = 0) and the right wall (X = L) for particles with a size of 1 and 10 micrometers is almost zero, which is due to the dominance of the buoyancy force over the drag and Brownian forces, while the particles with a size of 100 nm deposited on these walls due to the dominance of Brownian force.

In addition. as indicated in Figs. 7 and 8, as well as in the supplementary tables, a large number of particles with a size of 10 micrometers deposited at the bottom of the chamber due to gravitational force. On the other hand, according to Figs. 5 and 6, as the Rayleigh number increases, the strength of the vortices inside the chamber also increases. Since the flow direction in these vortices moves from the bottom to the top, some of the particles that are in the process of settling at the bottom are recirculated and do not settle. Therefore, the number of settled particles at the bottom of the chamber (which mostly occurs for particles of 10 micrometers) decreases. As a result, the number of settled particles for the larger-sized particles (10 micrometers) decreases with an increase in the Rayleigh number.

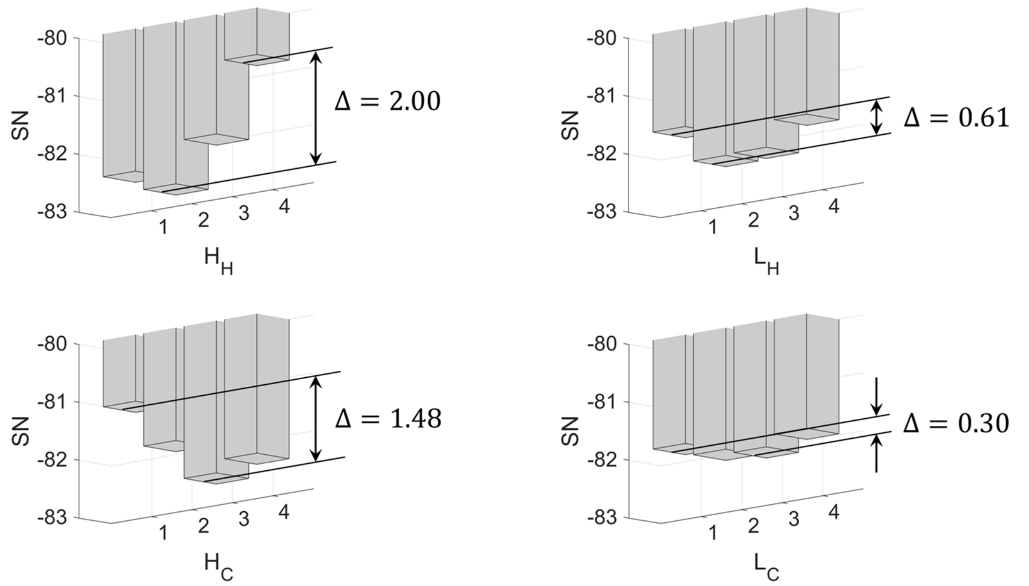

Fig. 9. The mean value of the SN ratio for different levels of each factor (Ra = 10^4, Size = 10 µm).

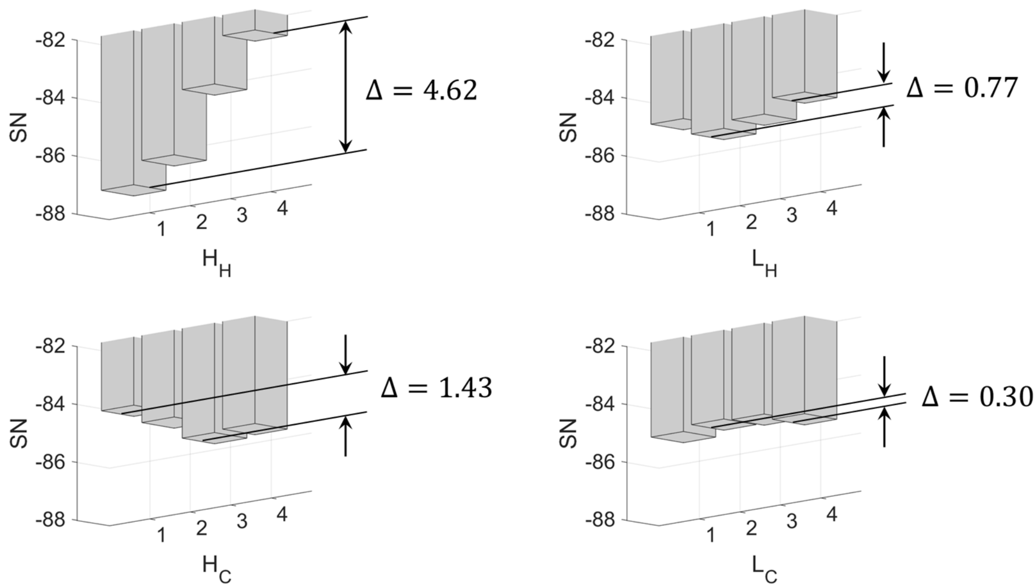

Fig. 10. The mean value of the SN ratio for different levels of each factor (Ra = 10^5, Size = 10 µm).

According to the obtained results, the location of the HC system does not have a significant effect on the deposition rate of small-sized particles (1 µm and 100 nm), but for particles with a size of 10 µm, where the most of the Covid-19 and Sars viruses are in this range, the effect of the HC system location is evident on the number of suspended particles. Therefore, the optimization will be done only for the particle with a size of 10 micrometers.

To find the optimal levels for the considered factors, the values of the SN ratio are first calculated according to the "smaller value is best" criterion. The SN ratio obtained from Taguchi analysis to achieve the reduction of suspended particles is shown in Figs. 9 and 10. A high value of the mean of the SN ratio for a level of a factor indicates that the desired level in our evaluation is in an optimal state. In other words, the optimal value of a factor is the value corresponding to the level in which the SN ratio is maximum. Therefore, according to Figs. 9 and 10, the optimal level of the considered factors for different Rayleigh numbers is stated in Table 6. Figures 11(a) and 11(b) show the flow pattern and Figs. 12(a) and 12(b) show the particles deposited on the walls for the optimized experiments of Taguchi analysis.

Table 6. Optimum level of each factor for different Rayleigh numbers.

Rayleigh number	Optimum Value				Number of Deposited Particles
	H_H	L_H	H_C	L_C	
Ra = 10^4	Level = 4 $X = 0.00$ $0.75 < Z < 1.00$	Level = 1 $X = 0.00$ $0.00 < Y < 0.25$	Level = 1 $X = 1.00$ $0.00 < Z < 0.25$	Level = 1 $X = 1.00$ $0.00 < Y < 0.25$	54605
Ra = 10^5	Level = 4 $X = 0.00$ $0.75 < Z < 1.00$	Level = 4 $X = 0.00$ $0.75 < Y < 1.00$	Level = 1 $X = 1.00$ $0.00 < Z < 0.25$	Level = 2 $X = 1.00$ $0.25 < Y < 0.50$	53373

Table 7. The mean value of the SN ratio and the importance of factors (Ra = 10^4, Size = 10 μm).

Level	H_H	L_H	H_C	L_C
1	−82.46	−81.69	−81.15	−81.88
2	−82.80	−82.31	−81.95	−82.10
3	−82.06	−82.29	−82.63	−82.18
4	−80.81	−81.84	−82.41	−81.98
Δ	2.00	0.61	1.48	0.30
Rank	1	3	2	4

Table 8. The mean value of the SN ratio and the importance of factors (Ra = 10^5, Size = 10 μm).

Level	H_H	L_H	H_C	L_C
1	−87.32	−85.04	−84.36	−85.27
2	−86.53	−85.62	−85.01	−85.08
3	−84.33	−85.37	−85.79	−85.15
4	−82.71	−84.85	−85.72	−85.38
Δ	4.62	0.77	1.43	0.30
Rank	1	3	2	4

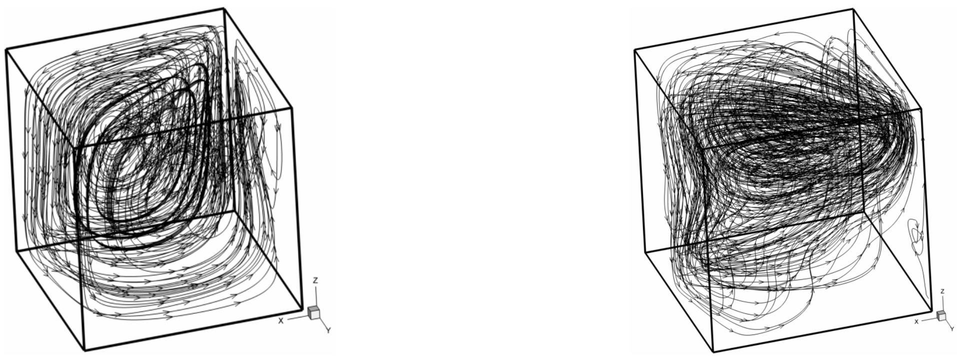

(a) (b)

Fig. 11. The flow pattern of the optimum experiment, (a) Ra = 10^4, (b) Ra = 10^5.

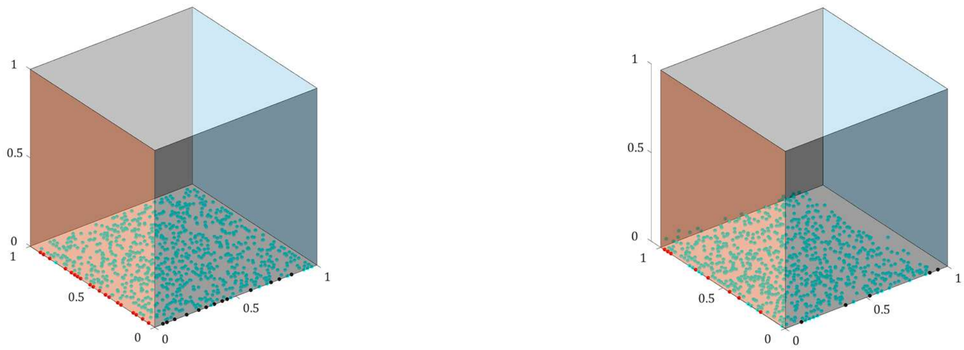

(a) (b)

Fig. 12. The pattern of deposited particles on the walls of the optimum experiment, (a) Ra = 10^4, (b) Ra = 10^5.

By performing statistical analysis, the importance of each factor in the issue of reducing suspended particles in the room can be easily determined. A summary of this statistical analysis is given in [25]. Table 7 and 8 show the numerical values of the SN ratio as well as the importance of each factor for two different Rayleigh numbers. Undoubtedly, more changes in the value of the SN ratio indicate a high degree of importance for each factor.

According to Tables 7 and 8, it can be seen that for both Rayleigh numbers 10^4 and 10^5, the height position of the heater system, H_H, is the most important factor and the longitudinal position of the cooler system, L_C, is the least important in the reduction of suspended particles in a room. Therefore, special importance should be given in choosing the location of the heating system for optimal ventilation in a room.

5. Conclusions

In this work, the effect of HC system location, which is based on natural heat convection, on particle deposition in a room has been studied by selecting various positions for the HC system. The number of deposited particles has been reported and Taguchi's optimization method is used to determine the best location for reducing the number of suspended particles. Regarding the presented results the following conclusions are drawn:

- The location of the HC system does not have a significant effect on the deposition rate of small-sized particles (1 μm and 100 nm)

- For particles with a size of 10 μm, where the most of the Covid-19 and Sars viruses are in this range, the effect of the HC system location is evident on the number of suspended particles.
- The best location for the heater to reduce the number of suspended 10 μm particles is: $0.75 < Z < 1.00$ and $0.00 < Y < 0.25$, $0.75 < Z < 1.00$ and $0.75 < Y < 1.00$ for $Ra = 10^4$ and $Ra = 10^5$, respectively.
- The best location for the cooler to reduce the number of suspended 10 μm particles is: $0.00 < Z < 0.25$ and $0.00 < Y < 0.25$, $0.00 < Z < 0.25$ and $0.25 < Y < 0.50$ for $Ra = 10^4$ and $Ra = 10^5$, respectively.
- The height position of the heater system, H_H, is the most important factor and the longitudinal position of the cooler system, L_C, is the least important to reduce the number of suspended particles.

The current study is based on a cubic room shape, which allows for symmetrical boundary conditions and a simplified flow pattern analysis. However, the model can be extended to other room shapes, such as rectangular, cylindrical, or L-shaped rooms, by adjusting the boundary conditions and reconfiguring the heating and cooling system (HC) placements.

In all cases, the governing equations of fluid motion and particle dynamics remain applicable, but the boundary conditions and initial conditions need to reflect the specific geometry. Optimization techniques such as the Taguchi method can still be employed to find the optimal HC system placement for different room geometries, ensuring effective particle deposition and contamination control.

While this study has successfully optimized the location of HC systems for minimizing suspended particles in enclosed environments, there are several areas for future research. First, the present study focused on natural convection heat transfer for HC systems; future studies could investigate forced convection systems or mix convection approaches to better understand their impact on particle deposition. Moreover, while Taguchi's optimization method allowed us to explore a range of parameters efficiently, further research using more optimization techniques such as RSM and GA or machine learning methods could provide deeper insights.

Author Contributions

H. Sajjadi planned the scheme, initiated the project, wrote the article draft, and analyzed the results; S.N. Nabavi analyzed the optimization results; A.A. Delouei developed the LBM method; M. Atashafrooz developed the DOE method. M.M. Rashidi analyzed the results and revised the article draft. The manuscript was written through the contribution of all authors. All authors discussed the results reviewed, edited, and approved the final version of the manuscript.

Acknowledgments

Not Applicable

Conflict of Interest

The authors declared no potential conflicts of interest concerning the research, authorship, and publication of this article.

Funding

The authors received no financial support for the research, authorship, and publication of this article.

Data Availability Statements

The datasets used and/or analyzed during the current study available from the corresponding author on reasonable request.

Appendix A

The number of deposited particles on each wall has been shown in Tables A.1 to A.6.

Table A.1. Number of 1 μm deposited particles on the various walls for different positions of the HC system and $Ra = 10^4$.

Number of Experiment	Left wall (X = 0)	Right wall (X = L)	Bottom wall (Z = 0)	Top wall (Z = H)	Behind wall (Y = 0)	Front wall (Y = L)
1	0	0	1579	0	0	0
2	0	0	1577	0	0	0
3	0	0	1576	0	0	0
4	0	0	1579	0	0	0
5	2	0	1600	0	0	0
6	1	0	1600	0	0	0
7	1	0	1600	0	0	0
8	1	0	1600	0	0	0
9	1	0	1600	0	0	0
10	1	0	1600	0	0	0
11	1	0	1603	0	0	0
12	1	0	1600	0	0	0
13	1	0	1600	0	0	0
14	1	0	1600	0	0	0
15	3	0	1600	0	0	0
16	1	0	1600	0	0	0

Table A.2. Number of 10 µm deposited particles on the various walls for different positions of the HC system and Ra = 10^4.

Number of Experiment	Left wall (X = 0)	Right wall (X = L)	Bottom wall (Z = 0)	Top wall (Z = H)	Behind wall (Y = 0)	Front wall (Y = L)
1	0	0	52643	0	0	0
2	0	0	50215	0	0	0
3	0	0	48967	0	0	0
4	0	0	50795	0	0	0
5	0	0	50901	0	0	0
6	0	0	51098	0	0	0
7	0	0	49285	0	0	0
8	0	0	49387	0	0	0
9	0	0	50903	0	0	0
10	0	0	50070	0	0	0
11	0	0	52363	0	0	0
12	0	0	51822	0	0	0
13	0	0	52799	0	0	0
14	0	0	52332	0	0	0
15	0	0	52840	0	0	0
16	0	0	54058	0	0	0

Table A.3. Number of 100 nm deposited particles on the various walls for different positions of the HC system and Ra = 10^4.

Number of Experiment	Left wall (X = 0)	Right wall (X = L)	Bottom wall (Z = 0)	Top wall (Z = H)	Behind wall (Y = 0)	Front wall (Y = L)
1	40	0	120	0	0	27
2	51	0	124	0	0	30
3	49	0	113	0	0	36
4	49	0	149	0	0	32
5	45	0	105	0	0	36
6	50	0	130	0	0	22
7	47	0	108	0	0	33
8	53	0	127	0	0	23
9	47	0	129	0	0	27
10	60	0	134	0	0	35
11	55	0	128	0	0	26
12	48	0	99	0	0	23
13	38	0	98	0	0	36
14	29	0	121	0	0	29
15	38	0	98	0	0	26
16	38	0	109	0	0	28

Table A.4. Number of 1 µm deposited particles on the various walls for different positions of the HC system and Ra = 10^5.

Number of Experiment	Left wall (X = 0)	Right wall (X = L)	Bottom wall (Z = 0)	Top wall (Z = H)	Behind wall (Y = 0)	Front wall (Y = L)
1	50	0	1535	0	0	7
2	62	0	1538	0	0	0
3	66	0	1514	0	0	0
4	52	0	1523	0	0	0
5	56	0	1629	0	0	4
6	58	0	1606	0	0	0
7	60	0	1600	0	0	0
8	64	0	1603	0	0	0
9	44	0	1603	0	0	3
10	60	0	1600	0	0	0
11	53	0	1623	0	0	0
12	54	0	1626	0	0	0
13	37	0	1600	0	0	0
14	42	0	1600	0	0	0
15	41	0	1619	0	0	0
16	41	0	1609	0	0	0

Table A.5. Number of 10 µm deposited particles on the various walls for different positions of the HC system and Ra = 10^5.

Number of Experiment	Left wall (X = 0)	Right wall (X = L)	Bottom wall (Z = 0)	Top wall (Z = H)	Behind wall (Y = 0)	Front wall (Y = L)
1	0	0	43186	0	0	0
2	1	0	40206	0	0	0
3	0	0	38720	0	0	0
4	2	0	40742	0	0	0
5	10	0	44499	0	0	0
6	7	0	43297	0	0	0
7	6	0	40574	0	0	0
8	11	0	42568	0	0	0
9	14	0	46121	0	0	0
10	7	0	45819	0	0	0
11	4	0	49547	0	0	0
12	3	0	48355	0	0	0
13	0	0	49930	0	0	0
14	0	0	49123	0	0	0
15	0	0	50137	0	0	0
16	0	0	52021	0	0	0

Table A.6. Number of 100 nm deposited particles on the various walls for different positions of the HC system and Ra = 10^5.

Number of Experiment	Left wall (X = 0)	Right wall (X = L)	Bottom wall (Z = 0)	Top wall (Z = H)	Behind wall (Y = 0)	Front wall (Y = L)
1	90	0	112	0	0	76
2	122	0	149	0	0	21
3	117	0	146	0	0	15
4	110	0	127	1	0	17
5	124	0	88	2	0	65
6	149	0	93	1	0	20
7	157	2	57	3	0	49
8	127	0	75	1	0	27
9	108	0	61	6	0	63
10	132	2	42	13	0	30
11	127	0	61	8	0	25
12	98	0	69	8	0	30
13	93	0	64	38	0	47
14	103	0	78	42	0	40
15	106	0	89	36	0	35
16	88	0	103	36	0	27

References

[1] Li, L., He, R., Kong, M., Eilts, S.M., Hong, J., Hogan, J., Pope, C.J., Effect of low-cost recirculating portable air filtration on aerosol particle deposition and concentration in a conference room: Experiment, theory, and simulation comparison, *Journal of Aerosol Science*, 166, 2022, 106048.
[2] Stadnytskyi, V., Bax, C.E., Bax, A., Anfinrud, P., The airborne lifetime of small speech droplets and their potential importance in SARSCoV-2 transmission, *Proceedings of the National Academy of Sciences of the United States of America*, 117(22), 2020, 11875-11877.
[3] Al Assaad, D., Ghali, K., Ghaddar, N., Shammas, E., Modeling of indoor particulate matter deposition to occupant typical wrinkled shirt surface, *Building and Environment*, 179, 2020, 106965.
[4] Sajjadi, H., Ahmadi, G., Amiri Delouei, A., Effect of inlet air locations on particle concentration using large eddy simulation based on multi relaxation time lattice Boltzmann method, *Journal of Applied and Computational Mechanics*, 7, 2021, 1944-1955.
[5] Al Assaad, D., Ghali, K., Ghaddar, N., Particles dispersion due to human prostration cycle and ventilation system in a prayer room, *Building and Environment*, 150, 2019, 44-59.
[6] Feng, Y., Marchal, Th., Sperry, T., Yi, H., Influence of wind and relative humidity on the social distancing effectiveness to prevent COVID-19 airborne transmission: A numerical study, *Journal of Aerosol Science*, 147, 2020, 105585.
[7] Haghighifard, H.R., Tavakol, M.M., Ahmadi, G., Numerical study of fluid flow and particle dispersion and deposition around two inline buildings, *Journal of Wind Engineering and Industrial Aerodynamics*, 179, 2018, 385-406.
[8] Keshavarz, S.A., Salmanzadeh, M., Ahmadi, G., Computational modeling of time resolved exposure level analysis of a heated breathing manikin with rotation in a room, *Journal of Aerosol Science*, 103, 2017, 117-131.
[9] Bektas, S., Senturk Lule, S., Colak, U., The computational fluid dynamics evaluation of the diffuser on N-16 radioisotope rise time in TRIGA mark II research reactor tanks, *Progress in Nuclear Energy*, 134, 2021, 103677.
[10] Worth Longest, P., Oldham, M.J., Mutual Enhancements of CFD Modeling and Experimental Data: A Case Study of 1-µm Particle Deposition in a Branching Airway Model, *Inhalation Toxicology*, 18, 2006, 761-771.
[11] Sajjadi, H., Salmanzadeh, M., Ahmadi, G., Jafari, S., Lattice Boltzmann method and RANS approach for simulation of turbulent flows and particle transport and deposition, *Particuology*, 30, 2017, 62-72.
[12] Sajjadi, H., Salmanzadeh, M., Ahmadi, G., Jafari, S., Investigation of particle deposition and dispersion using Hybrid LES/RANS model based on Lattice Boltzmann method, *Scientia Iranica*, 25(6), 2018, 3173-3182.
[13] Sajjadi, H., Salmanzadeh, M., Ahmadi, G., Jafari, S., Simulations of indoor airflow and particle dispersion and deposition by the lattice Boltzmann method using LES and RANS approaches, *Building and Environment*, 102, 2016, 1-12.
[14] Zhao, B., Zhang, Z., Li, X., Numerical study of the transport of droplets or particles generated by respiratory system indoors, *Building and Environment*,

40, 2005, 1032–1039.
[15] Liu, S., Novoselac, A., Transport of Airborne Particles from an Unobstructed Cough Jet, *Aerosol Science and Technology*, 48, 2014, 1183–1194.
[16] Ahmadzadeh, M., Shams, M., A numerical approach for preventing the dispersion of infectious disease in a meeting room, *Scientific Reports*, 12, 2022, 1-25.
[17] Muthusamy, J., Haq, S., Akhtar, S., Alzoubi, M.A., Shamim, T., Alvarado, J., Implication of coughing dynamics on safe social distancing in an indoor environment—A numerical perspective, *Building and Environment*, 206, 2021, 108280.
[18] Kochenderfer, M.J., Wheeler, T.A., *Algorithms for optimization*, MIT Press, 2019.
[19] Montgomery, D.C., *Design and analysis of experiments*, John Wiley & Sons, 2017.
[20] Woo, M.W., Daud, W.R.W., Tasirin, S.M., Talib, M.Z.M., Optimization of the spray drying operating parameters—A quick trial-and-error method, *Drying Technology*, 25(10), 2007, 1741-1747.
[21] Maier, H.R., Razavi, S., Kapelan, Z., Matott, L.S., Kasprzyk, J., Tolson, B.A., Introductory overview: Optimization using evolutionary algorithms and other metaheuristics, *Environmental Modelling & Software*, 114, 2019, 195-213.
[22] Slowik, A., Kwasnicka, H., Evolutionary algorithms and their applications to engineering problems, *Neural Computing and Applications*, 32, 2020, 12363-12379.
[23] Schiefer, H., Schiefer, F., *Statistics for Engineers: An Introduction with Examples from Practice*, 2021.
[24] Kechagias, J.D., Aslani, K.E., Fountas, N.A., Vaxevanidis, N.M., Manolakos, D.E., A comparative investigation of Taguchi and full factorial design for machinability prediction in turning of a titanium alloy, *Measurement*, 151, 2020, 107213.
[25] Karna, S.K., Sahai, R., An overview on Taguchi method, *International Journal of Engineering and Mathematical Sciences*, 1(1), 2012, 1-7.
[26] Davis, R., John, P., Application of Taguchi-based design of experiments for industrial chemical processes, Statistical approaches with emphasis on design of experiments applied to chemical processes, 2018.
[27] Sajjadi, H., Nabavi, S.N., Atashafrooz, M., Delouei, A.A., Optimization of Heating and Cooling System Locations by Taguchi's Method to Maximize or Minimize the Natural Convection Heat Transfer Rate in a Room, *Iranian Journal of Science and Technology, Transactions of Mechanical Engineering*, 47, 2023, 1599-1614.
[28] Maghsoodloo, S., The exact relation of Taguchi's signal-to-noise ratio to his quality loss function, *Journal of Quality Technology*, 22(1), 1990, 57-67.
[29] Sajjadi, H., Amiri Delouei, A., Mohebbi, R., Izadi, M., Succi, S., Natural convection heat transfer in a porous cavity with sinusoidal temperature distribution using Cu/water nanofluid: Double MRT lattice Boltzmann method, *Communications in Computational Physics*, 29, 2021, 292-318.
[30] Sajjadi, H., Amiri Delouei, A., Atashafrooz, M., Effect of magnetic field on particle deposition in a modeled room, *Particulate Science and Technology*, 41, 2023, 361-370.
[31] Khanafer, K., Vafai, K., Lightstone, M., Buoyancy-driven heat transfer enhancement in a two-dimensional enclosure utilizing nanofluids, *International Journal of Heat and Mass Transfer*, 46, 2003, 3639-3653.

ORCID iD

H. Sajjadi https://orcid.org/0000-0002-0681-7682
S.N. Nabavi https://orcid.org/0000-0002-1531-8957
A.A. Delouei https://orcid.org/0000-0001-7414-4195
M. Atashafrooz https://orcid.org/0000-0001-7063-4509
M.M. Rashidi https://orcid.org/0000-0002-6309-8688

How to cite this article: Sajjadi H. et al., Optimization and Sensitivity Analysis of Location Parameters in Heating and Cooling Systems for Minimizing Suspended Particles in an Enclosed Environment, *J. Appl. Comput. Mech.*, 11(3), 2025, 692-706. https://doi.org/10.22055/jacm.2024.47488.4725